Automatic segmentation of mitochondria in EM data using pairwise affinity factorization and graph-based contour searching

Ovidiu Ghita, Julia Dietlmeier, *Member, IEEE*, and Paul F. Whelan, *Senior Member, IEEE*

Abstract—**In this paper we investigate the segmentation of closed contours in sub-cellular data using a framework that primarily combines the pairwise affinity grouping principles with a graph partitioning contour searching approach. One salient problem that precluded the application of these methods to large scale segmentation problems is the onerous computational complexity required to generate comprehensive representations that include all pairwise relationships between all pixels in the input data. To compensate for this problem a practical solution is to reduce the complexity of the input data by applying an over-segmentation technique prior to the application of the computationally demanding strands of the segmentation process. This approach opens the opportunity to build specific shape and intensity models that can be successfully employed to extract the salient structures in the input image which are further processed to identify the cycles in an undirected graph. The proposed framework has been applied to the segmentation of mitochondria membranes in electron microscopy (EM) data which are characterized by low contrast and low signal to noise ratio. The algorithm has been quantitatively evaluated using two datasets where the segmentation results have been compared with the corresponding manual annotations. The performance of the proposed algorithm has been measured using standard metrics such as Precision and Recall and the experimental results indicate a high level of segmentation accuracy.**

***Index Terms*—Mitochondria segmentation, electron microscopy, affinity models, spectral clustering and graph searching.**

Manuscript received December 19, 2013. This work was supported by the National Bio-Photonics and Imaging Platform (NBIP) Ireland funded under the Higher Education Authority PRTLI Cycle 4, co-funded by the Irish Government and the European Union - /Investing in your future/.

Ovidiu Ghita is with the Centre for Image Processing and Analysis (CIPA), School of Electronic Engineering, Dublin City University, Dublin 9, Ireland (phone: +353-1-7007637; fax: +353-1-7005508; e-mail: ghitao@ eeng.dcu.ie).

Julia Dietlmeier, Paul F. Whelan are with the Centre for Image Processing and Analysis (CIPA), School of Electronic Engineering, Dublin City University, Dublin 9, Ireland (e-mail: julia.dietlmeier2@mail.dcu.ie, paul.whelan@dcu.ie).

I. INTRODUCTION

The accurate segmentation of mitochondria in microscopy images represents a challenging research topic that is motivated by the biological importance of these membrane-enclosed sub-cellular organelles. Mitochondria are substructures of the cells with sizes ranging from 0.5 to 10 μm and their primary role is the processing of the food molecules into adenosine triphosphate (ATP) which provides energy for the cells. In addition to the generation of ATP, mitochondria play an important role in several cellular functions such as signaling, differentiations, cell growth and mitochondrial regulation processes [1-3] and a substantial number of studies were focused on the investigation of the cellular mechanisms that regulate the mitochondrial shapes and their links to specific cellular functions and mitochondrial diseases [4]. In this sense, mitochondria present substantial morphological variations which correspond to different cellular states which are in particular noticeable during mitochondrial fusion and fission processes [2]. In addition to shape variations that normally occur during the cellular life, substantial morphological changes in the structure of mitochondria are also caused by disturbances caused by cellular perturbations [2,5].

Sub-cellular imaging is commonly performed using electron microscopy (EM) modalities which have sufficient resolution to image organelles such as mitochondria [7]. The interpretation of EM mitochondria data presents a challenging process in scientific studies due to two main issues. The first issue is associated with the vast amount of data that is generated by the EM modality, while the second problem is given by the presence of numerous non-mitochondrial structures, high level of noise and substantial intensity variations. These two problems gained substantial prominence in clinical studies as the interpretation of the EM mitochondria data involves manual segmentation, which proved to be an extremely laborious and time consuming task. The labor intensive characteristic of the manual annotation process is detailed in [8]. In this analysis the researchers use semi-automatic software tools such as IMOD [9] and CellProfiler [10] and the exhaustive analysis of the EM mitochondria may require several months [8]. These limitations raised several questions in regard to the practicality of the manual annotation of the EM mitochondria data and a recent direction of research investigates the application of pattern recognition and statistical machine learning methods for automatic mitochondria segmentation. While the use of computer vision solutions for mitochondria identification in sub-cellular data answers a demanding clinical problem, the development of such automatic segmentation algorithms provides a challenging task. This conclusion is

motivated by several factors which include computational issues that are generated by the volume of data to be processed, wide range of shapes and textures that are associated with mitochondria which can be easily confused with other sub-cellular structures such as membranes and vesicles, severe intensity variations and low signal to noise ratio. It is important to mention that these challenges vary to a great extent depending on the type of cells that are analysed and the development of automatic mitochondria segmentation is currently an open area of research.

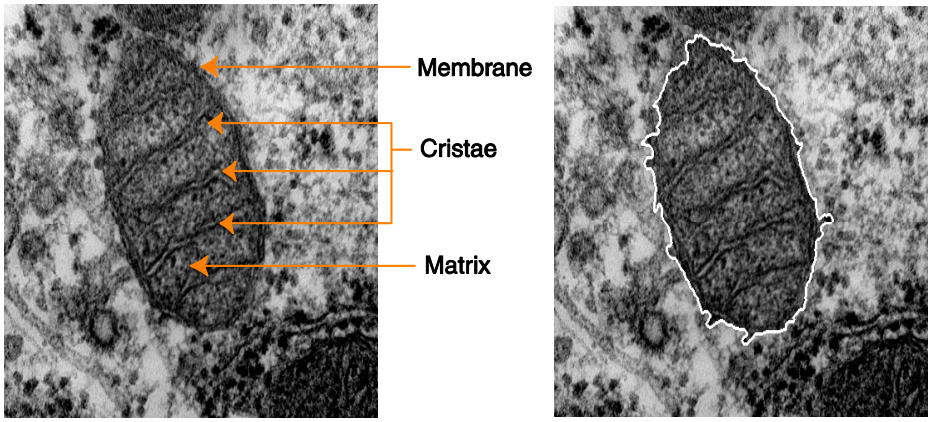

Fig. 1. Mitochondrial structure. The left image illustrates the main components of a mitochondrion [6]. The right image presents the segmentation results obtained after the application of the proposed segmentation algorithm that is described in Section II. Note the highly cluttered background and the low intensity contrast that is specific for mitochondria EM data.

The main hypothesis that was employed in the development of computer vision solutions for mitochondria segmentation is based on the observation that these sub-cellular organelles are defined by closed structures with distinct inner textures (see Fig. 1). Thus, two main directions of research emerged that attempted to exploit specific knowledge in relation to the morphology and/or structural characteristics of mitochondria [33]. In this regard, a good example of this line of approach is represented by the work of Narasimha et al [11] where they proposed a texton-based algorithm for mitochondria detection which involves the joint classification using k-NN, support vector machines (SVM) and adaptive boosting (AdaBoost). This approach has been applied to the segmentation of mitochondria in MNT-1 cells and they conclude that their method performs similar and in some situations better than semi-automatic techniques based on level sets. A similar idea is followed in [12] where the authors employed the standard Gabor filtering method in conjunction with a Gentle-Boost classifier to detect mitochondria in rat brain tissues. The reported experiments indicate relative large misclassifications (false acceptance rate is 25% and false

rejection rate is 20%) and this fact highlights two major disadvantages associated with the texture-based methods: the complexity of the training process and the fact that these approaches are poorly equipped to adapt to changes in the *cristae* structure (*cristae* are folds of the inner mitochondrial membrane) that are induced by cellular and mitochondria membrane events [3].

To counteract the limitations associated with structure-based segmentation methods when applied to mitochondria segmentation, alternative approaches based on active contours [5,13] and graph partitioning [1,14,15] have been proposed. Active contours methods in particular proved successful when deployed in the implementation of semi-supervised segmentation algorithms, but they have shown to be impractical when applied in conventional forms to mitochondria EM data. This is caused by several issues such as difficulty in obtaining accurate contour initialization, weak gradients caused by low intensity profiles that are often characteristic for mitochondria membranes, random textures, noise, and more importantly difficulties in deriving statistical models that precisely encompass the modes of variation of the mitochondria shapes. To mitigate these limitations Seyedhosseini et al [7] combined the use of algebraic curves and texture to identify image patches that resemble mitochondria which are later ranked by a random forest classifier. They have tested their algorithm on mouse neuropil and Drosophila VNC data and they report promising results. In an effort to redress the problems associated with traditional level sets implementations when used for segmentation of sub-cellular structures, Nguyen and Ji [16] initially embedded the watershed segmentation into an energy minimization framework (watersnake) and then they incorporate prior information in the form of fixed and variable shape terms that constrain the space that is spanned during the contour propagation process. They quantitatively evaluated their algorithm on rat liver mitochondria data and they demonstrated that the inclusion of prior shape information proved a key element in achieving accurate segmentation results. In spite of these performance improvements the use of active contours for mitochondria segmentation proved problematic due to contour initialization errors and a large set of parameters that require optimization. Therefore, these approaches were successful when applied to cellular data where the range of mitochondria shapes varies within a restricted domain.

This limitation was recently addressed by the application of graph partitioning algorithms to mitochondria segmentation and the guiding idea was to identify the cycles corresponding to mitochondria contours in undirected graphs. This is usually obtained by enforcing shape minimization constraints to an undirected graph where the nodes

are defined in most simplistic cases by pixels or in more involved approaches by adjacent regions resulting from a pre-segmentation step. Building on this idea, Lucchi et al [1,14] combined a primary segmentation step that involves the calculation of superpixels with a graph cut algorithm where unary and pairwise potentials of an energy function were employed to incorporate shape cues that are inferred by SVM classification. While graph partitioning techniques are better equipped than active contour-based methods for the segmentation of sub-cellular structures they have several practical issues. The first problem relates to the complexity of the undirected graphs in which closed contours are detected and the second (and perhaps the most difficult problem to tackle) is the inference of graph searching constraints that accurately encode a set of rules that allows the identification of mitochondria membranes when dealing with the noisy and low contrast nature of the EM data. These issues form the main research problems that are addressed in this paper and it is our conviction that these challenges can be elegantly and efficiently answered by an algorithm that combines pairwise affinity grouping principles with graph partitioning techniques. The proposed algorithm provides an attractive segmentation framework as it facilitates the implementation of an automated solution that is able to adapt to the large diversity of the mitochondria shapes in highly cluttered environments that are characteristic for EM data.

This paper is organized as follows. Section II starts with a brief overview of the proposed segmentation method which is continued by a detailed presentation of all computational strands of the algorithm. Section III includes a discussion about experimental results and compares the performance achieved by the proposed segmentation method when applied to mitochondria segmentation with the results reported for other related implementations. Section IV provides concluding remarks that highlight the main findings that emerge from this investigation and outlines the future directions of research.

II. Overview of the Proposed Method

The proposed segmentation method consists of a multi-stage scheme in which the first step involves data pre-processing whose aim is twofold, to reduce the noise and to enhance the local structure coherence. To reduce the complexity of the input data, the second step of the algorithm applies the technique detailed in [17] which over-segments the data in superpixels, which are image patches with similar intensity characteristics. This reduction in data complexity allows the application of a spectral clustering algorithm where targeted association rules between

superpixels are factored into a similarity model which encompasses the intensity and spatial properties of the mitochondria membranes. The resulting similarity model encapsulates specific saliency models into an affinity matrix and the extraction of the salient features implies the calculation of the leading eigenvector from which are derived sets of discrete clusters. The output of the spectral clustering algorithm generates the primary mitochondria segmentation which consists of a set of connected superpixels that require additional processing stages to accurately identify the mitochondria membranes. To facilitate further contour processing, an undirected graph is constructed which encodes the spatial relationships between the superpixels resulting from the spectral clustering step. Then a standard graph searching approach is applied to identify the cycles in the undirected graph structure. From this information, the mitochondria contour is identified by enforcing intensity minimization constraints. The last step of the algorithm applies contour post-processing which aims to correct the localization errors in the estimation of the superpixels which are caused by the low gradients that are associated with mitochondria membranes. The complete processing pipeline is presented in Fig. 2 and full details related to each step of the proposed segmentation algorithm will be presented in the remainder of this section.

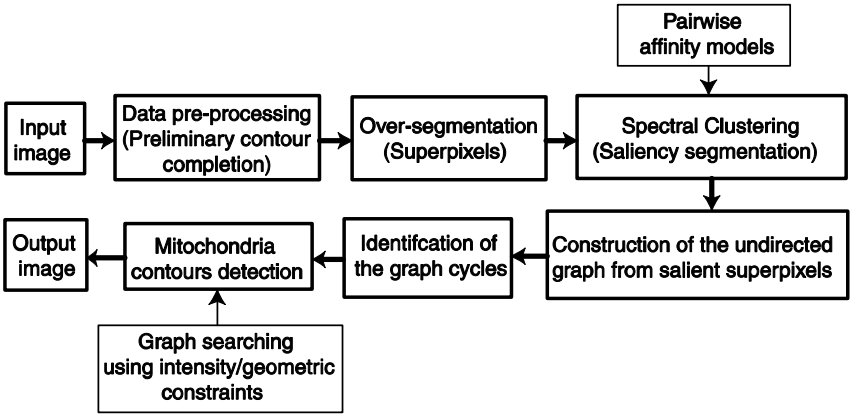

Fig. 2. Overview of the mitochondria segmentation algorithm.

A. Data Pre-processing Step

The high level of noise and the low intensity contrast between mitochondria membranes and background are distinct characteristics of the EM data. Thus, the first step of the algorithm, as illustrated in Fig. 2, applies a data pre-processing procedure to improve the coherence of the local structures and contextual information (i.e. enhancement of directional consistent (or flow-like) patterns) in the input data. The goal of this pre-processing step is to improve the contour completion using directional filters which involves an approach related to the coherence anisotropic

diffusion process proposed by Weickert in [18]. The filtering scheme detailed in [18] enhances the directional structures in the image with respect to the local orientation computed from the structure tensor and a version of this algorithm has been applied by Tasdizen et al [34] to improve the contrast in transmission EM images. In this paper, we have replaced the iterative anisotropic diffusion smoothing scheme in [18] with the application of directional Gaussian kernels [19,20] to implement a more scalable feature enhancement process that allows better regularization (i.e. contour gap completion) along flow-like structures. This is motivated by two reasons. Firstly, the directional Gaussian filters provide a wider non-linear spatial averaging than the anisotropic process, which allows better contour completion when dealing with larger gaps in the local structure, and secondly this approach involves a non-iterative scheme which has clear advantages in the presence of high levels of noise by decoupling the *scale* of the noise from the *scale* of the contour gaps that need to be bridged by the enhancement of the oriented features in the image. As the use of directional Gaussian filters requires knowledge in relation to local orientation, the first step of the data enhancement (pre-processing) step involves the calculation of the integrated structure tensor $J\rho$ (for clarity reasons we have used the same notations used in [18]),

$$J_\rho = K_\rho * \left(\nabla u_\sigma \nabla u_\sigma{}^T\right), \ \rho, \sigma \in R^+ \tag{1}$$

where K_ρ denotes the Gaussian filter with the scale parameter ρ and ∇u_σ is the convolution of the input image with the first derivative of the Gaussian filter with the scale parameter σ. In (1) ρ is a spatial integration coefficient that controls the neighbourhood over which the structure tensor is calculated and σ is a parameter chosen in relation to the level of noise present in the image. The increased spatial domain where the structure tensor is calculated allows the estimation of the local orientation θ within the neighbourhood $N(\rho)$. The structure tensor is defined by a symmetric matrix and the local orientation θ is given by the orientation of the eigenvector e that corresponds to the smallest eigenvalue, $e = (\cos(\theta), \sin(\theta))^T$. The local orientation θ is calculated for each pixel in the image and the pre-processed image is obtained by convolving the input image with a bank of directional filters as follows,

$$\begin{aligned} &v(x,y) = u(x,y) * g(x,y,\sigma_x,\sigma_y,\theta), \ \ (x,y) \in \Omega, \ \sigma_x << \sigma_y \\ &g(x,y,\sigma_x,\sigma_y,\theta) = \frac{1}{2\pi\sigma_x\sigma_y} \exp\left(-\left(\frac{[x\cos(\theta) + y\sin(\theta)]^2}{2\sigma_x^2} + \frac{[-x\sin(\theta) + y\cos(\theta)]^2}{2\sigma_y^2} \right) \right) \end{aligned} \tag{2}$$

where u is the input image, v is the enhanced image, σ_x, σ_y are the scale parameters that parameterize the shape of the directional filter and Ω is the image domain. To implement a anisotropic kernel with orientation θ we need to constrain $\sigma_x << \sigma_y$.

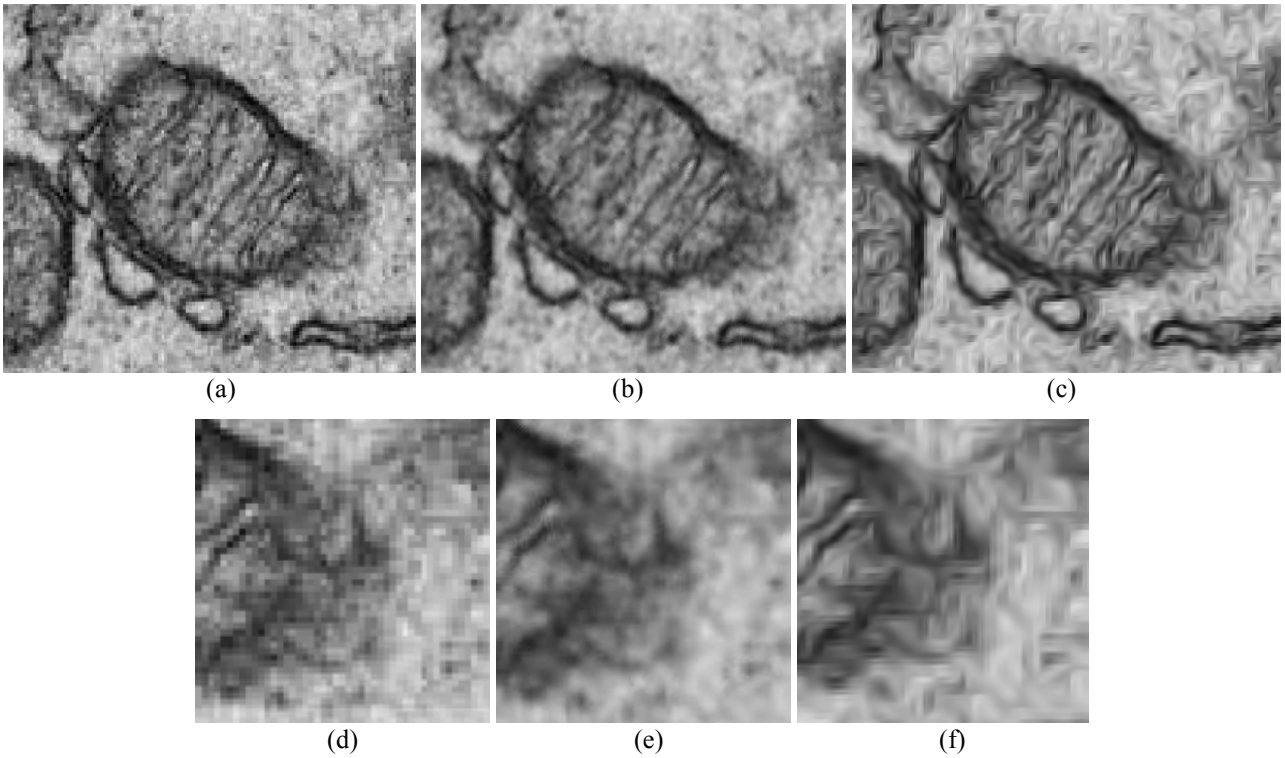

Fig. 3. Data pre-processing results. (a) Original EM image. (b) Image enhancement using our directional filtering method that is described in Section II.A (parameters ρ=4.0, σ=1.0, σ_x=0.5, σ_y=4.0). (c) Image enhancement using coherence enhancing anisotropic diffusion [18] (parameters: ρ=4.0, σ=1.0, Δt=0.15, t=3). (d-f). Close-up details corresponding to images (a-c). Note that the proposed data enhancement scheme avoids the introduction of artificial flow-like structures in the enhanced image that is one of the drawbacks associated with the coherence enhancing anisotropic diffusion algorithm.

An example that illustrates the application of the pre-processing step is depicted in Fig. 3. To highlight the advantages associated with the proposed algorithm when applied to the enhancement of EM mitochondria data shown in Fig. 3 we also include the enhanced image obtained by the coherence enhancing anisotropic diffusion (CEAD) algorithm detailed in [18]. In Fig. 3 it can be observed that both algorithms succeed in enhancing the oriented features in the image but the CEAD algorithm achieves this advantage at the expense of inserting artificial flow-like structures in the output image. These extraneous structural artefacts are caused in part by the image noise but more frequently by regularization errors that are caused by the limited spatial domain that is processed by the coherence-enhancing diffusion around each pixel in the image. As shown in Fig. 3(e), the proposed algorithm avoids

the insertion of undesired flow-like structures and this advantage is motivated by two factors. Firstly, the proposed algorithm involves a non-iterative scheme which avoids error propagations that occur in the presence of noise and weak contours, and secondly the directional filters implement a more accurate filtering process when compared to the anisotropic diffusion process. To allow a direct comparison between the image enhancement strategy discussed in this section and the CEAD algorithm the parameters used in the calculation of the structure tensor J_ρ are set to the same values ρ=4.0 and σ=1.0 for both algorithms.

B. Over-segmentation Step

One difficult issue that restricts the application of graph partitioning algorithms to large scale segmentation problems is the complexity of the input data. Encoding all pixel relationships in the input data using graph representations leads to very large data structures that are not feasible to be used for practical segmentation tasks. To circumvent this computational bottleneck, the input data is either downscaled or tiled into equally sized subsections on which the developed algorithm is sequentially applied. There is no doubt that these solutions are not effective when applied to complex segmentation tasks due to the difficulty of imposing coherent shape and intensity constraints. An alternative to this approach is the development of over-segmentation algorithms that generate a primary partition of the input data into regions or image patches with similar intensity characteristics. In this regard, a large range of over-segmentation algorithms have been proposed to date [17,21,22] where the main quest was obtaining image regions or superpixels with uniform texture or intensity properties. In this paper we have applied the SLIC algorithm proposed in [17] which generalize the k-means algorithm. This method starts with an initial number of seed locations which are iteratively enlarged into superpixels with respect to connectivity and *a priori* size constraints until a convergence criterion is met. Full details about this algorithm are provided in [17].

The main advantage of this algorithm over alternative implementations based on the watershed transform [23] is the regularized tessellation of the input image that is given by the lattice of superpixels. An illustration of the output of this algorithm when applied to a selection of mitochondria images is presented in Fig. 4. These primary segmentation results provide a substantial reduction in the complexity of the input image and they facilitate the application of the computationally demanding processes related to spectral clustering and graph partitioning. These steps relate to the major contributions that emerge from this investigation and will be detailed in Section II.C.

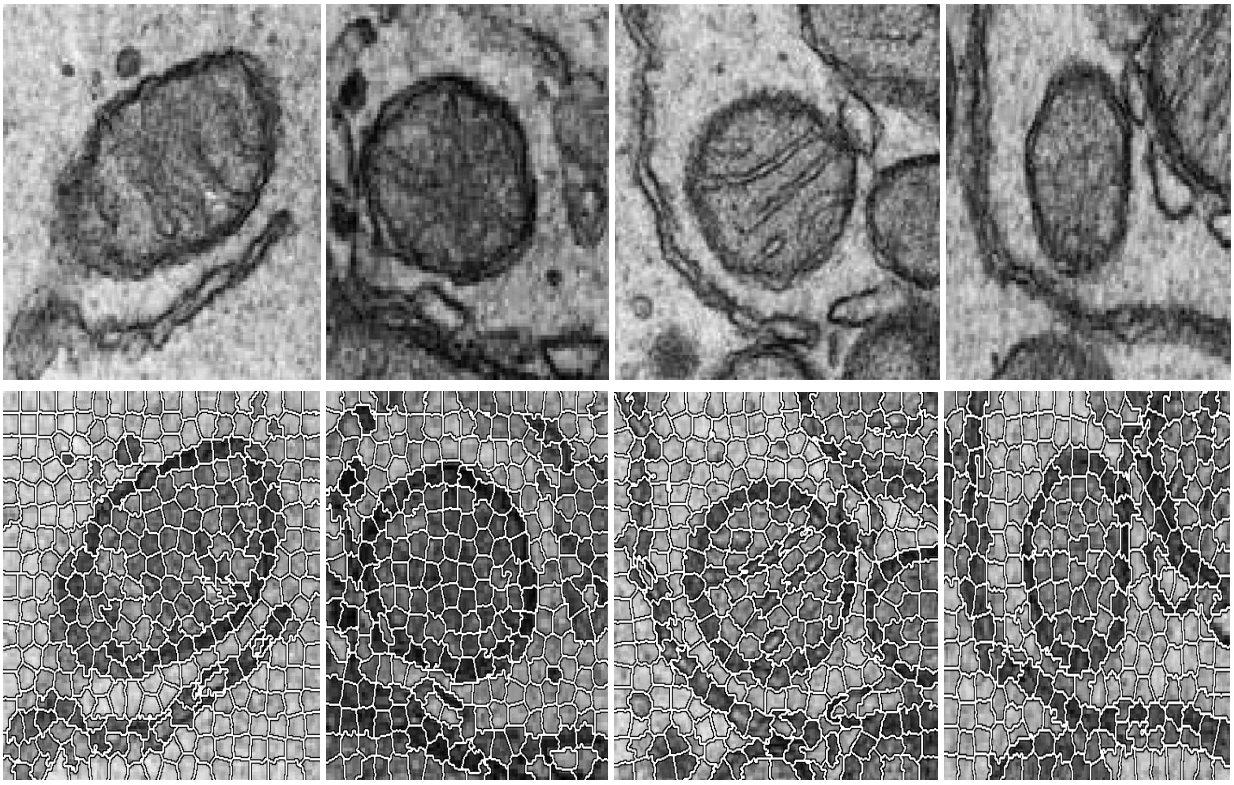

Fig. 4. Results detailing the application of the over-segmentation procedure on a selection of mitochondria images. (Top row) Input images. (Bottom row) Over-segmented images showing the borders of the superpixels.

C. Segmentation Process

The proposed segmentation process entails three distinct computational strands. The first step implements a primary segmentation and operates on the lattice of superpixels that are determined in the over-segmentation stage. The aim of this computational step is to implement a foreground cut algorithm which is based on the concept of pairwise affinity [24]. More precisely, the goal is to obtain an affinity factorization by computing the affinity matrix which encapsulates the relationships between all pairs of superpixels in the image with respect to predefined grouping criteria such as closeness in the intensity and spatial domains. Then, from the affinity matrix the global salient and non-salient structures can be determined by means of spectral clustering (which implies the evaluation of the eigen spectrum of the affinity matrix). To facilitate the calculation of the affinity matrix for all superpixels we need to calculate their mean intensity values and their centroids. After this, we need to define similarity or affinity function(s) that will be applied in the calculation of pairwise relationships that are entries in the affinity matrix A,

where A_{ij} represents the similarity between the superpixels $(i, j) \in \Omega$. For the purpose of grouping the superpixels into a saliency structure that approximates the mitochondria contours, we define the following affinity functions:

$$F_1(i,j) = \exp(-\frac{I(i)+I(j)}{2a_1^2})$$
$$F_2(i,j) = \exp(-\frac{|I(i)-I(j)|}{2a_2^2}) \quad (3)$$
$$F_3(i,j) = \exp(-\frac{dist(c_i, c_j)}{2a_3^2})$$

where $I(i)$ and c_i are the mean intensity and the centroid of the superpixel with index i. These three functions return values in the interval (0,1] and they implement low level properties that encode the intensity and spatial constraints that are characteristic for mitochondria contours. In this regard, the function F_1 implements the constraint that the superpixels associated with mitochondria contours are defined by low intensity values, the function F_2 enforces an intensity continuity constraint (i.e. F_2 returns values closer to 1.0 when the mean intensity values of the superpixels i and j are similar) and finally the function F_3 implements a spatial continuity constraint that assigns larger values for superpixels whose distance between their centroids c_i and c_j is small. The parameters a_1, a_2 and a_3 are parameters that weigh the strength of each constraint in the calculation of the affinity matrix A and the intensity values and superpixel distances are normalised in the range [0,1]. If the number of superpixels in the image is N then the affinity matrix is $N \times N$ and is calculated as follows,

$$A_{ij} = F_1(i,j)F_2(i,j)F_3(i,j), \quad A_{ii} = 1, \quad (i,j) \in \Omega \quad (4)$$

It can be observed that the affinity matrix A calculated in (4) is symmetric and its entries have large values for pairs of superpixels that respond strongly to the conditions implemented by the three affinity functions shown in (3). Since the number of superpixels in the over-segmented image is N, which is a value substantially smaller than the number of pixels in the input image, the calculation of the eigenvectors for A represents a computationally tractable eigen-decomposition problem, $A = P\Lambda P^T$ where $P = [p_1, p_2 \ldots p_N]$ is the eigenvectors matrix and Λ is the matrix that contains the eigenvalues λ_i ($\lambda_1 > \lambda_2 \ldots > \lambda_N$) corresponding to eigenvectors $p_i | i \in [1, N]$. Since the best L_2 approximation of the affinity matrix A is given by the multiplication of the most significant eigenvector p_1 with the squared value of the largest eigenvalue λ_1 [24], the extraction of global salient features that are consistent with the properties encoded

by the three affinity functions entails the application of a standard data partitioning process to p_1 using either k-means or multi-class thresholding. As A is symmetric, the elements of the eigenvector p_1 take values in the interval (0,1] and the salient superpixels with respect to (3) correspond to the largest values in p_1. Based on experimentation we discovered that the superpixels associated with complete (closed) mitochondria contours are situated in the highest quartile of the values of the eigenvector p_1 and the partition of p_1 has been carried out using the multi-level Otsu classification [25]. Results of the spectral clustering algorithm when applied to the mithocondria images shown in Fig. 4 are presented in Fig. 5.

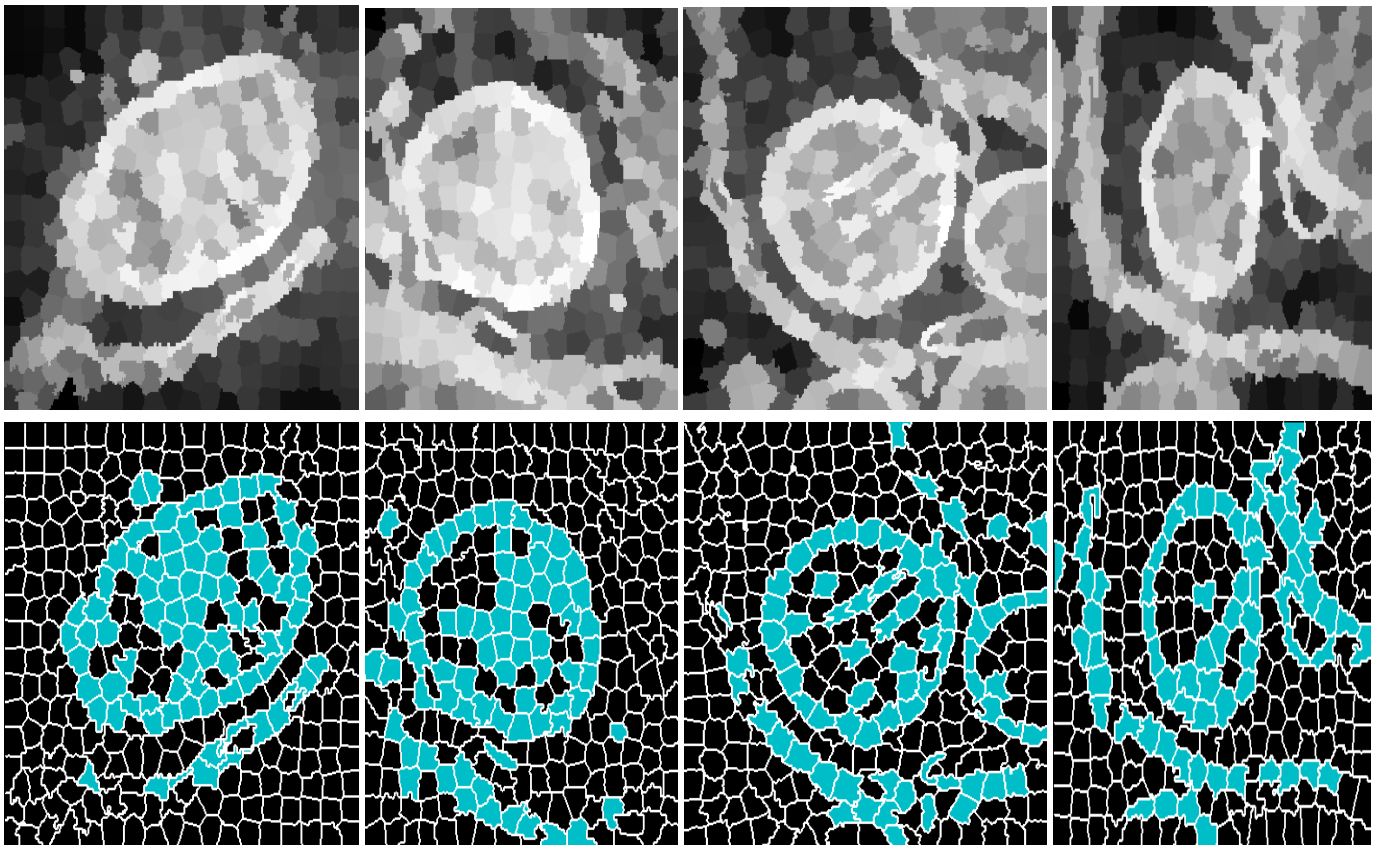

Fig. 5. Spectral clustering results obtained when the algorithm has been applied to the images depicted in Fig. 4. (Top row) The most significant eigenvector p_1 that is calculated from the affinity matrix A (for visualization purposes the values of the elements of p_1 are mapped using 256 grayscale levels). (Bottom row) Spectral clustering results obtained from the Otsu classification. The superpixels that form the preliminary segmentation map are highlighted in light blue. The affinity matrix is calculated using the saliency rules detailed in (3) and the parameters a_1, a_2 and a_3 are set to the following values, 0.8,1.0 and 1.0 respectively.

The application of the spectral clustering process, as illustrated in Fig. 5, generates primary segmentation results that incorporate intensity and shape continuity constraints, but these results do not provide precise segmentations as they embed only global saliency rules. In spite of these imperfections, the use of spectral clustering is opportune as it further reduces the complexity of the input data by dramatically reducing the number of superpixels that require further analysis. This fact allows the application of graph partitioning methods that can be employed to identify the cycles in an undirected graph that correspond to mitochondria membranes. To this end, the cycles in the undirected graph (whose nodes are the superpixels contained in the primary segmentation results) are detected using the breadth-first search algorithm (BFS) [26] using the following pseudocode sequence:

$$
\begin{aligned}
&G(\mathrm{V},\mathrm{E}) - \text{is the undirected graph, } \mathrm{V} = \{\mathrm{v_i}\}, i \in [1, S], \mathrm{E} \subset \mathrm{V} \times \mathrm{V} \\
&\text{Identify all cycles in } \mathrm{G(V,E)}: \\
&\text{for } \forall\, \mathrm{v_i} \mid i \le S \text{ and } \mathrm{v_k} \mid \exists\, \mathrm{E_m} = \{\mathrm{v_i}, \mathrm{v_k}\}, \ell = \mathrm{BFS}(\mathrm{v_i}, \mathrm{v_k}) \\
&\text{if } \ell \neq \{\mathrm{v_i}, \mathrm{v_k}\} \text{ add } \ell \text{ to the path list } \Psi \\
&\text{if the number of paths in } \Psi = \mathrm{q} \\
&\ell_{\mathrm{m}} = \arg\min_{s}\left(s = \frac{I(\ell_q)}{card(\ell_q)}\right)\Big|\ell_{\mathrm{q}} \in \Psi
\end{aligned}
\tag{5}
$$

The algorithm described synthetically in (5) identifies all cycles in the graph G(V,E) where V = $\{v_i\}$ denotes the S nodes associated with the salient superpixels determined by the spectral clustering algorithm and E are the edges that are two-element subsets of V that encode the links between the connected nodes in G. The BFS algorithm is applied to pairs of nodes (v_i,v_k) for which an edge E_m= {v_i, v_k} exists. If the BFS algorithm returns a non-trivial path (i.e. different than the set {v_i,v_k}) it is included in the path list Ψ. From all the paths (cycles) in the list Ψ, the mitochondrion path ℓ_m is given by the path that minimizes an intensity constraint with respect to the cardinality (the number of nodes) of the paths ℓ_q in Ψ. The superpixels contained in the output path ℓ_m allow the extraction of the mitochondria contours. These contours are post-processed using the GAC active contour method [27,28] to compensate for the boundary errors associated with the superpixels in areas with low contrast between the mitochondria contours and background.

$$
\frac{\partial \Phi}{\partial t} = |\nabla \Phi| div\left(g(\nabla v)\left(\frac{\nabla \Phi}{|\nabla \Phi|}\right)\right) + \beta |\nabla \Phi| g(\nabla v) \tag{6}
$$

$$
\Phi(t = 0, x, y) = \Phi_0(\ell_m) \tag{7}
$$

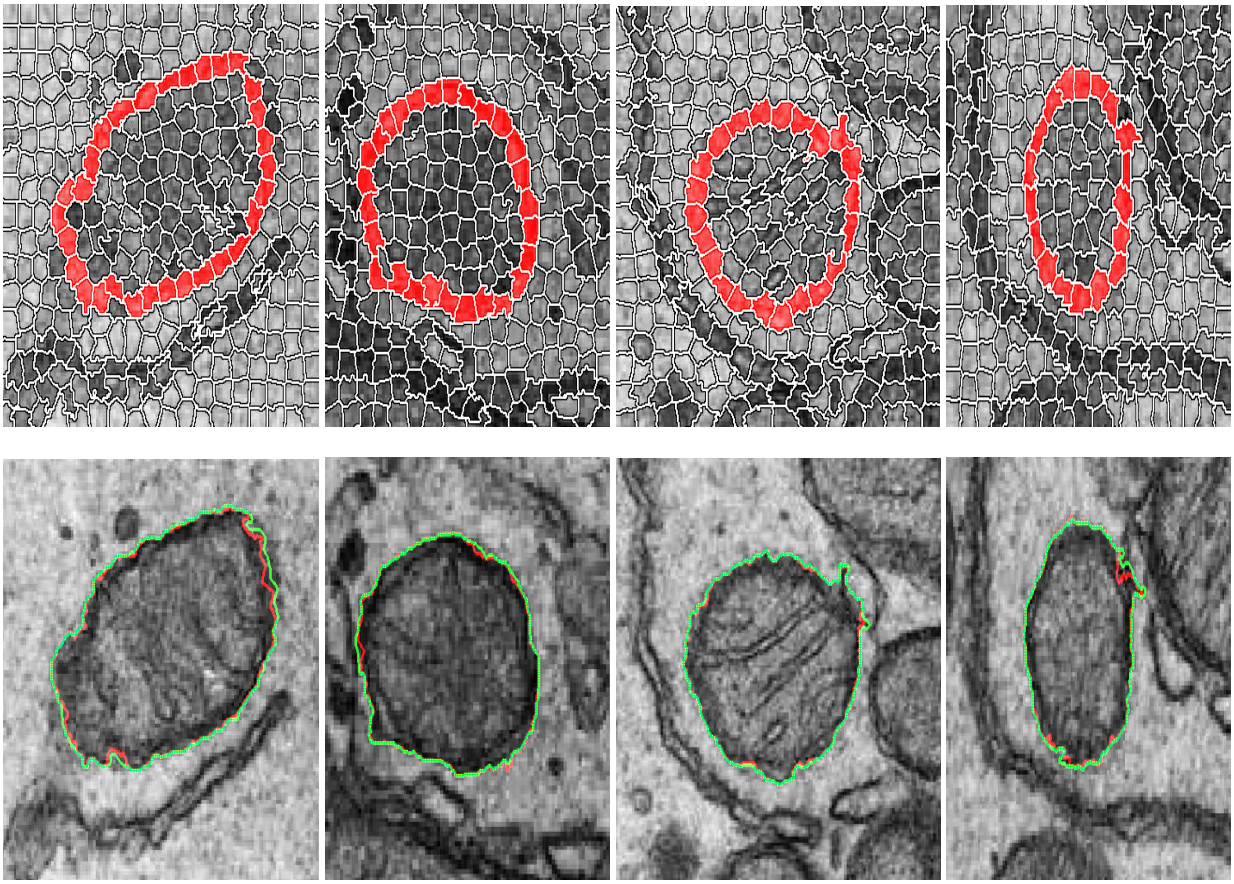

Fig. 6. Mitochondria segmentation results for images depicted in Fig. 4. (Top row) Results after the application of the graph searching process (see equation 5 for details). (Bottom Row) Final segmentation results (The mitochondria contours resulting from the graph searching process are displayed in red. In green are shown the post-processed mitochondria contours obtained after the application of the GAC algorithm). This diagram is best viewed in color.

III. Experimental Results

The experiments were conducted using two mitochondria EM datasets. The first database of EM images has been provided by the American Society of Cell Biology (ASCB). This database consists of 20 images detailing mitochondria in ductulus efferens of the ground squirrel cells [29]. The second dataset comprises 30 serial section transmission EM images of the Drosophila first instar larva ventral nerve cord (VNC) [35,36]. Mitochondria in both cell lines have a wide selection of shapes varying from elongated to circular and inhomogeneous *cristae* structures. In addition to these changes in the morphology of mitochondria, a predominant characteristic of these images is the substantial variation in the intensity signal between the mitochondria membranes and the background and the occurrence of shadow effects that are caused by the limited resolution of the EM images. The parameters for the

proposed algorithm were presented in Section II and they have been used unchanged in all experiments presented in this section. The two datasets that were used in the experimental analysis have been constructed by extracting sub-images from the original data that comprise complete mitochondria structures.

TABLE I. PERFORMANCE METRICS THAT WERE USED TO VALIDATE THE PROPOSED SEGMENTATION ALGORITHM.

Performance measures	Mathematical expression
Accuracy	(TP+TN)/(TP+TN+FP+FN)
Precision	TP/(TP+FP)
Recall	TP/(TP+FN)
F-score	2.0*Precision*Recall/(Precision + Recall)
VOC	TP/(TP+FP+FN)

The accuracy of the proposed method has been tested against manual annotations that were validated by an experienced biologist and in this process we employed a range of performance metrics to evaluate the agreement between the manual segmentations and the results returned by the proposed method. The first set of experimental results are reported for Drosophila VNC data due to the fact that this dataset is publicly available and consequently it provides an ideal point of comparison between our method and other segmentation approaches. To quantify the performance of the segmentation process we calculated a set of performance metrics such as Accuracy, Precision, Recall, F-score and VOC (see Table I) that were previously used in the evaluation of other mitochondria segmentation algorithms. Table II includes the experimental results for our approach and three segmentation methods that were also evaluated using the Drosophila VNC data (Seyedhosseini et al [7], RLF [31] and Giuly et al [13]).

TABLE II. SEGMENTATION RESULTS OBTAINED FOR OUR METHOD AND OTHER MITOCHONDRIA SEGMENTATION TECHNIQUES THAT WERE EVALUATED USING THE DROSOPHILA VNC DATASET.

	Accuracy	Precision	Recall	F-score	VOC
Seyedhosseini et al [7]	-	0.78	0.68	0.72	-
RLF [31]	-	0.46	0.57	0.51	-
Giuly et al [13]	-	0.64	0.57	0.60	-
Proposed method	0.95 ± 0.02	0.95 ± 0.05	0.85 ± 0.08	0.89 ± 0.05	0.81 ± 0.07

The quantitative results presented in Table II show the better performance obtained by the proposed algorithm when compared to alternative methods based on curve propagation and patch classification. While these experimental

results are important as they sample in detail the performance obtained by our method when applied to challenging EM data, we feel that a more inclusive comparison with other mitochondria segmentation approaches that are evaluated on EM data acquired from different cell lines would allow us not only to broaden the scope of this investigation but also to help us to analyze the proposed algorithm in the wider context of mitochondria segmentation. In this regard, experimental results for additional mitochondria segmentation algorithms including the works of Lucchi et al [1], Nguyen and Ji [16], Seyedhosseini et al [7], Fulkerson [30], RLF [31] and TextonBoost [32] are reported in Table III.

TABLE III. ADDITIONAL MITOCHONDRIA SEGMENTATION RESULTS REPORTED FOR EM DATA ACQUIRED FROM DIFFERENT CELL LINES.

	Cell line	Accuracy	Precision	Recall	F-score	VOC
TextonBoost [32]	hippocampus	0.95	-	-	-	0.61
Fulkerson [30]	hippocampus	0.96	-	-	-	0.69
Learned-f [1]	hippocampus	0.98	-	-	-	0.82
Learned-f [14]	striatum	-	-	-	-	0.74
Nguyen and Ji [16]	frozen-hydrated rat liver	-	0.95	0.70	-	-
RLF [31]	mouse neuropil	-	0.78	0.82	0.80	-
Seyedhosseini et al [7]	mouse neuropil	-	0.82	0.82	0.82	-
Proposed method ASCB dataset	ductulus efferens	0.97 ± 0.01	0.94 ± 0.03	0.96 ± 0.01	0.95 ± 0.01	0.91 ± 0.02

While a direct compassion between the results presented in Table III is difficult, as they were reported for data captured from different cells lines using different image acquisition protocols, they are convergent on the fact that the current range of mitochondria segmentation methods are well able to achieve high levels of true positives (TP) but this is generally obtained at the expense of relative large numbers of false positives (FP) and false negatives (FN). While also achieving comparable TP rates in line with the best performing mitochondria segmentation methods, the proposed approach detailed in Section II returns low rates of FP and FN (this is emphasized by the VOC results which indicates that the highest scores are achieved by the proposed method and the Learned-f segmentation approach that is described in [1,14]). To complement the numerical results presented in Tables II and III with visual results, segmentation examples obtained by the proposed algorithm when applied to the ASCB and Drosophila VNC datasets are presented in Fig. 7 and Fig. 8, respectively.

The last element of this experimental study addresses the computational complexity of the proposed mitochondria segmentation algorithm. Computational times for each component of the processing pipeline (please

refer to Section II for details) are reported in Table IV and it can be observed that the most computationally intensive parts of the algorithm are associated with data pre-processing, spectral clustering and the GAC contour post-processing step (the algorithm was executed on a computer with a single core Intel 1.7GHz processor).

TABLE IV. AVERAGE COMPUTATIONAL COST FOR EACH COMPONENT OF THE PROPOSED ALGORITHM.

	Drosophila VNC	**ASCB**
Data pre-processing	3.89s	25.09s
SLIC superpixels	0.35s	2.76s
Spectral clustering	5.06s	7.46s
Graph searching	0.015s	0.15s
GAC post-processing	3.90s	14.76s

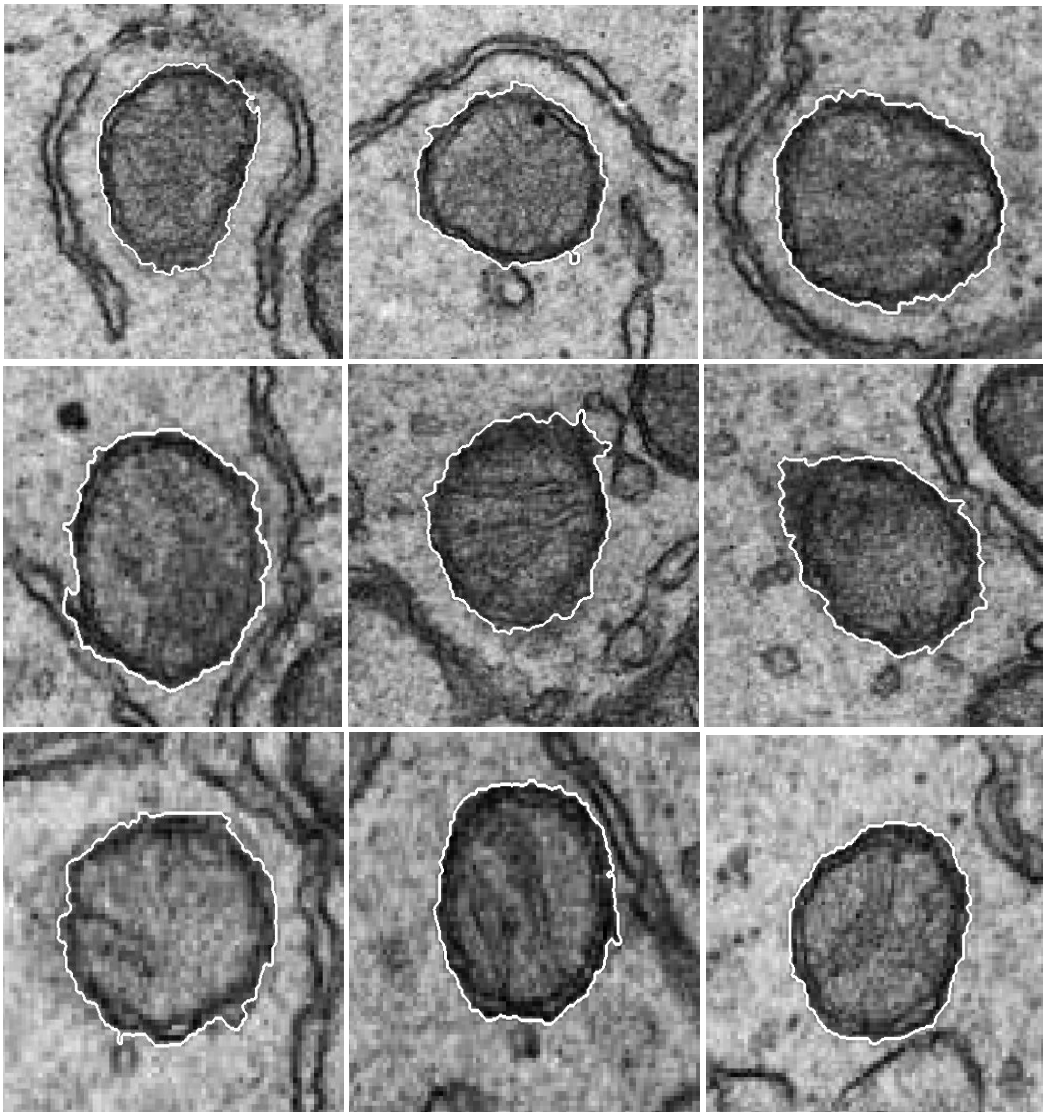

Fig. 7. Sample mitochondria segmentation results (ASCB dataset).

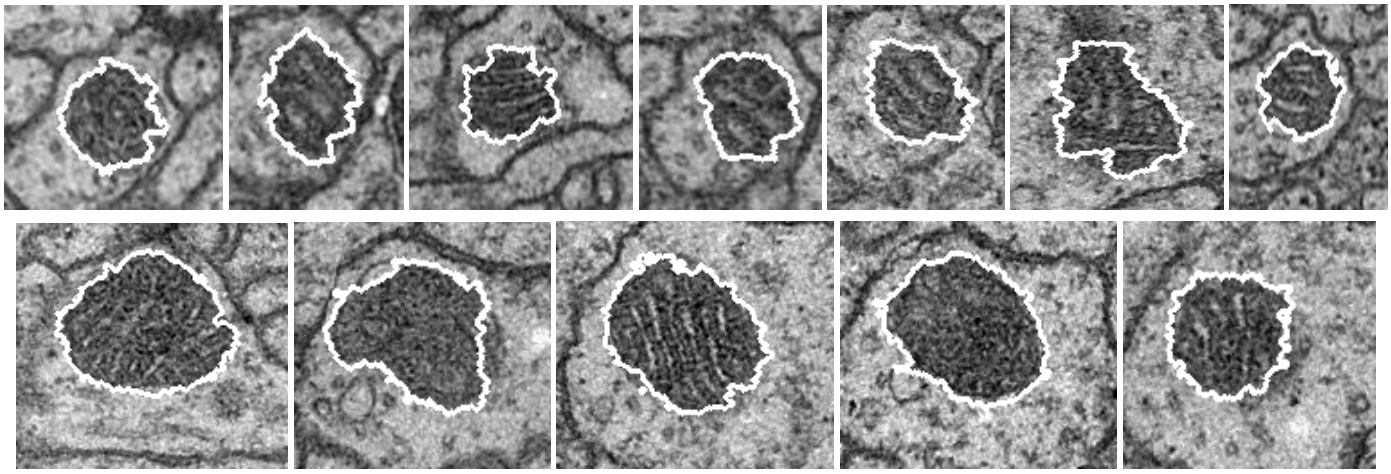

Fig. 8. Sample mitochondria segmentation results (Drosophila VNC dataset).

IV. CONCLUSIONS

The major objective of this paper was to introduce a new image processing pipeline that has been designed to adapt to the challenging scenario associated with the identification of mitochondria membranes in EM data. The proposed approach involves a multi-step segmentation scheme which couples the pairwise affinity factorization with a graph searching method that is applied to find the cycles in an undirected graph. To circumvent the computational bottleneck associated with the calculation of the eigen spectrum of the affinity matrix and the computational requirements associated with the construction of the undirected graph that encodes the pairwise relationships between all pixels in the input image, the first step of the algorithm applies a pre-segmentation steps that involves the identification of the regions in the image with similar intensity characteristics. This facilitates the application of the proposed technique to large segmentation problems and we have demonstrated the accuracy of our method when applied to mitochondria segmentation in EM data. Our experiments highlighted one distinct advantage associated with our method when compared to related mitochondria segmentation techniques, the low levels of false positive and false negatives in the final results. This advantageous property is motivated by the absence of complex training procedures that are typically applied to construct *a priori* models for mitochondria shapes or textures and/or the derivation of customized energy functionals that are able to guide the contour propagation process when dealing with the complex nature of the EM data. The largely unsupervised characteristic of the proposed segmentation technique presents another important advantage and our future studies will explore the application of the

segmentation method described in this paper to other medical imaging tasks. Another area of future work will address the generalization of this technique to adapt to multi-contour segmentation problems.

REFERENCES

[1] A. Lucchi, K. Smith, R. Achanta, V. Lepetit, and P. Fua, "A fully automated approach to segmentation of irregularly shaped cellular structures in EM images", in Proc of *Medical Image Computing and Computer Assisted Intervention* (MICCAI), pp. 463-471, 2010.

[2] D.C. Chan, "Mitochondria: dynamic organelles in disease, aging, and development", *Cell*, 125(7), pp. 1241–1252, 2006.

[3] K.G. Hales, "Mitochondrial Fusion and Division", *Nature Education*, 3(9), pp. 12, 2010.

[4] Y. Reis, M. Bernardo-Faura, D. Richter, T. Wolf, B. Brors, A. Hamacher-Brady, R. Eils, and N.R. Brady, "Multi-parametric analysis and modeling of relationships between mitochondrial morphology and apoptosis", *PLoS ONE*, 7(1): e28694, doi:10.1371/journal.pone.0028694, 2012.

[5] E.U. Mumcuoglu, R. Hassanpour, S.F. Tasel, G. Perkins, M.E. Martone, and M.N. Gurcan, "Computerized detection and segmentation of mitochondria on electron microscope images", *Journal of Microscopy*, 246(3), pp. 248-265, 2012.

[6] http://remf.dartmouth.edu/imagesindex.html. Accessed November 14th, 2013.

[7] M. Seyedhosseini, M. Ellisman, and T. Tasdizen, "Segmentation of mitochondria in electron microscopy images using algebraic curves", in *Proc. of the 10th IEEE International Symposium on Biomedical Imaging* (ISBI), pp. 860-863, 2013.

[8] A.B. Noske, A.J. Costin, G.P. Morgan, and B.J. Marsh, "Expedited approaches to whole cell electron tomography and organelle mark-up in situ in high-pressure frozen pancreatic islets", *Journal of Structural Biology*, 161(3), pp. 298-313, 2008.

[9] J.R. Kremer, D.N. Mastronarde, and J.R. McIntosh, "Computer visualization of three-dimensional image data using IMOD", *Journal of Structural Biology*, 116(1), pp. 71-6, 1996.

[10] A.E. Carpenter, T.R. Jones, M.R Lamprecht, C. Clarke, I.H. Kang, O. Friman, D.A. Guertin, J.H Chang, R.A. Lindquist, J. Moffat, P. Golland, and D.M. Sabatini, "CellProfiler: image analysis software for identifying and quantifying cell phenotypes", *Genome Biology*, 7(10), pp. R100, 2006.

[11] R. Narasimha, H. Ouyang, A.G. Gray, S.W. McLaughlin, and S. Subramaniam, "Automatic joint classification and segmentation of whole cell 3D images*", Pattern Recognition*, 42(6), pp. 1067-1079, 2009.

[12] S. Vitaladevuni, Y. Mishchenko, A. Genkin, D. Chklovskii, and K. Harris, "Mitochondria detection in electron microscopy images", in *Proc of the 3rd Workshop on Microscopic Image Analysis with Applications in Biology*, New York, USA, 2008.

[13] R. Giuly, M.E. Martone, and M.H. Ellisman, "Method: Automatic segmentation of mitochondria utilizing patch classification, contour pair classification, and automatically seeded level sets", *BMC Bioinformatics*, 13:29 doi:10.1186/1471-2105-13-29, 2012.

[14] A. Lucchi, K. Smith, R. Achanta, G. Knott, and P. Fua, "Supervoxel-based segmentation of mitochondria in EM image stacks with learned shape features", *IEEE Transactions on Medical Imaging*, 31(2), pp. 474-486, 2012.

[15] V. Thong Ta, O. Lezoray, A. Elmoataz, and S. Schüpp, "Graph-based tools for microscopic cellular image segmentation", *Pattern Recognition*, 42(6), pp. 1113-1125, 2009.

[16] H. Nguyen and Q. Ji, "Shape-driven three-dimensional watersnake segmentation of biological membranes in electron tomography*", IEEE Transactions on Medical Imaging*, 27(5), pp. 616-628, 2008.

[17] R. Achanta, A. Shaji, K. Smith, A. Lucchi, P. Fua, and S. Süsstrunk, "SLIC superpixels compared to state-of-the-art superpixel methods", *IEEE Transactions on Pattern Analysis and Machine Intelligence*, 34(11), pp. 2274 - 2282, 2012.

[18] J. Weickert, "Coherence-enhancing diffusion filtering", *International Journal of Computer Vision*, 31(2-3), pp. 111-127, 1999.

[19] V. Lakshmanan, "A separable filter for directional smoothing", *IEEE Geoscience and Remote Sensing Letters*, vol. 1, pp. 192-195, 2004.

[20] D. Charalampidis, "Efficient directional Gaussian smoothers", *IEEE Geoscience and Remote Sensing Letters*, 6(3), pp. 383-387, 2009.

[21] M. Van den Bergh, X. Boix, G. Roig, B. de Capitani, and L. Van Gool, "SEEDS: Superpixels extracted via energy-driven sampling", in *Proc. of European Conference on Computer Vision* (ECCV), pp. 13-26, 2012.

[22] A. Levinshtein, A. Stere, K.N. Kutulakos, D.J. Fleet, S.J. Dickinson, and K. Siddiqi, "TurboPixels: Fast superpixels using geometric flows", *IEEE Transactions on Pattern Analysis and Machine Intelligence*, 31(12), pp. 2290-2297, 2009.

[23] L. Vincent and P. Soille, "Watersheds in digital spaces: An efficient algorithm based on immersion simulations", *IEEE Transactions on Pattern Analysis and Machine Intelligence*, 13(6), pp. 583-598, 1991.

[24] P. Perona and W.T. Freeman, "A factorization approach to grouping", in *Proc. of European Conference on Computer Vision* (ECCV), pp. 655-670, 1998.

[25] P.S. Liao and P.C. Chung, "A fast algorithm for multilevel thresholding"*, Journal of Information Science and Engineering*, 17(5): 713-727, 2001.

[26] T.H. Cormen, C.E. Leiserson, R.L. Rivest, and C. Stein, *Introduction to Algorithms*, 3rd edition, The MIT Press, ISBN: 9780262533058, 2009.

[27] V. Caselles, R. Kimmel, and G. Sapiro, "Geodesic active contours", *International Journal of Computer Vision*, 22(1), pp. 61–79, 1997.

[28] C. Li, C. Gui, and M.D. Fox, "Distance regularized level set evolution and its application to image segmentation", *IEEE Transactions on Image Processing*, 19(2), pp. 3243-3254, 2010.

[29] The American Society for Cell Biology, http://www.ascb.org.

[30] B. Fulkerson, A. Vedaldi, and S. Soatto, "Class segmentation and object localization with superpixel neighborhoods", in *Proc. of the International Conference on Computer Vision* (ICCV), pp. 670-677, 2009.

[31] R. Kumar, A.V. Reina, and H. Pfister, "Radon-like features and their application to connectomics", in *Proc. of the Computer Vision and Pattern Recognition Workshops* (CVPRW), pp. 186-193, 2010.

[32] J. Shotton, J. Winn, C. Rother, and A. Criminisi, "Textonboost for image understanding: Multi-class object recognition and segmentation by jointly modeling texture, layout, and context", *International Journal of Computer Vision*, 81(1), pp. 2-23, 2009.

[33] J. Dietlmeier, O. Ghita, H. Duessmann, J.H. Prehn and P.F. Whelan, "Unsupervised mitochondria segmentation using recursive spectral clustering and adaptive similarity models", *Journal of Structural Biology*, 184(3), pp. 401-408, 2013.

[34] T. Tasdizen, R.T. Whitaker, R.E. Marc and B.W. Jones, "Enhancement of cell boundaries in transmission Electron Microscopy images," in *Proc. of the International Conference on Image Processing* (ICIP), vol. 2, pp. 129-132, 2005.

[35] A. Cardona, S. Saalfeld, S. Preibisch, B. Schmid, A. Cheng, J. Pulokas, P. Tomancak, V. Hartenstein, "An integrated micro- and macroarchitectural analysis of the Drosophila brain by computer-assisted serial section Electron Microscopy", *PLoS Biology*, 8(10): e1000502, 2010.

[36] Drosophila VNC Dataset: http://www.ini.uzh.ch/~acardona/data.html

Ovidiu Ghita received the BE and ME degrees in Electrical Engineering from Transilvania University, Brasov, Romania and the Ph.D. degree from Dublin City University, Ireland. From 1994 to 1996 he was an Assistant Lecturer in the Department of Electrical Engineering at Transilvania University. Since then he has been a member of the Vision Systems Group (VSG) at Dublin City University (DCU) and currently he holds a position of DCU-Research Fellow. Dr. Ghita has authored and co-authored over 90 peer-reviewed research papers in areas of instrumentation, range acquisition, machine vision, texture analysis and medical imaging.

Julia Dietlmeier received her Dipl.-Ing.(FH) degree in Electrical Engineering with the specialization in Wireless Communication from Munich University of Applied Sciences, Munich, Germany. She completed her Master of Science degree in Electrical and Computer Engineering from Portland State University, Portland, Oregon, USA where she was also working as a Teaching and a Research Assistant. From 1999 to 2001 she was employed as a R&D Engineer within Siemens Mobile Radio Division, Ulm, Germany where she was involved in the pilot UMTS base station project. Currently she is a full-time research assistant within the Centre for Image Processing and Analysis, Dublin, Ireland while working part-time on the completion of her Ph.D degree. Her research interests involve pattern analysis, statistical communication theory, information-theoretical problems and applied numerical methods. She is a member of IEEE and European Society for Molecular Imaging (ESMI).

Paul F. Whelan (S'84–M'85–SM'01) received his B.Eng. (Hons) degree from NIHED, M.Eng. degree from the University of Limerick, and his Ph.D. (Computer Vision) from Cardiff University, UK. During the period 1985-1990 he was employed by Industrial and Scientific Imaging Ltd and later Westinghouse (WESL), where he was involved in the research and development of high-speed computer vision systems. He was appointed to the School of Electronic Engineering, Dublin City University (DCU) in 1990 and is currently Professor of Computer Vision (Personal Chair). Prof. Whelan founded the Vision Systems Group (VSG) in 1990 and the Centre for Image Processing & Analysis (CIPA) in 2006 and currently serves as its director.

As well as publishing over 170 peer reviewed papers, Prof. Whelan has co-authored 2 monographs and co-edited 3 books. His research interests include image segmentation, and its associated quantitative analysis with applications in computer/machine vision and medical imaging. He is a Senior Member of the IEEE, a Chartered Engineer and a fellow of the IET. He served as a member of the governing board (1998-2007) of the *International Association for Pattern Recognition* (IAPR) and President (1998-2007) of the *Irish Pattern Recognition and Classification Society* (IPRCS). Prof. Whelan is a HEA-PRTLI (RINCE, NBIP) and Enterprise Ireland funded principal investigator.